Comp. Appl. Math. (2014) 33:147–161
DOI 10.1007/s40314-013-0052-4

Improved spherical continuation algorithm with application to the double-bounded homotopy (DBH)

D. Torres-Muñoz · H. Vazquez-Leal · L. Hernandez-Martinez · A. Sarmiento-Reyes

Received: 27 May 2013 / Accepted: 30 May 2013 / Published online: 21 June 2013

Abstract The homotopy continuation methods are useful tools for finding multiple solutions of nonlinear problems. An important issue of this kind of method is the correct implementation of the path-following techniques used to trace the homotopy trajectory. Therefore, in this work we propose a modification of the spherical algorithm to successfully trace the closed paths of a DBH homotopy. The proposed methodology is depicted with three examples. Finally, a comparison of the results with a standard path-following technique is presented and discussed.

Keywords Homotopy continuation methods · Multiple operating points

Mathematics Subject Classification 34A12 · 34A34

1 Introduction

The DC analysis is an important task for analyzing electrical circuits. This analysis consists of solving a system of nonlinear algebraic equations (NAEs) formulated using the

Communicated by Cristina Turner.

D. Torres-Muñoz (✉) · L. Hernandez-Martinez · A. Sarmiento-Reyes
National Institute for Astrophysics, Optics and Electronics,
Sta. María Tonantzintla, Puebla, México
e-mail: deletsm@gmail.com; dtorres@inaoep.mx

L. Hernandez-Martinez
e-mail: luish@inaoep.mx

A. Sarmiento-Reyes
e-mail: jarocho@inaoep.mx

H. Vazquez-Leal
School of Electronic Instrumentation and Atmospheric Sciences,
University of Veracruz, Xalapa, Veracruz, México
e-mail: hvazquez@uv.mx

Kirchhoff laws (Vazquez-Leal et al. 2011; Melville et al. 1993; Vazquez-Leal et al. 2013). Newton–Raphson (NR) is the most employed method to solve the NAEs due to the quadratic convergence rate (Ogrodzki 1994). Nonetheless, NR may fail to converge to a solution unless the initial estimation point is close enough to the solution. Therefore, homotopy continuation methods (HCM) are proposed as an alternative to the NR method. What is more, HCM methods are capable of locating multiple operating points, which have applications in the analysis of multistable circuits.

The basic idea of the HCM methods is to embed a homotopy parameter λ into the NAES, yielding to a continuous deformation from a trivial state to the nonlinear state (Melville et al. 1993; Watson et al. 1997; Dyes et al. 1999; Vazquez-Leal et al. 2013, 2012). Such procedure can be represented by

$$H : R^{n+1} \longrightarrow R^n, \quad x \in R^n \quad \text{and} \quad \lambda \in [0, 1], \tag{1}$$

where n is the number of variables in the system and x represents circuit electrical variables. The last equation satisfies the following conditions:

(1) If $\lambda = 0$, then $H(x, 0) = 0$ has a trivial or known solution.
(2) If $\lambda = 1$, then $H(x, 1) = F(x)$ has the solution of the original NAEs.

Several homotopy formulations have been reported as the Newton homotopy (NH) (Wu 2006), the fixed point homotopy (FPH) (Yamamura et al. 1999), multiparameter homotopy (Wolf and Sanders 1996; Vazquez-Leal et al. 2011) and double-bounded homotopy (DBH) (Vazquez-Leal et al. 2005). Among them, the DBH homotopy is highlighted by its stop criterion.

In general, the success of homotopy simulation depends on factors such as:

- Several homotopy formulations are reported in the literature with different characteristics. Therefore, the proper selection of a homotopy is a key factor to the success of finding multiple operating points.
- A suitable path-following technique is required for an accurate path tracking of the homotopy trajectories. Otherwise, the homotopy simulation can suffer from ill conditions for tracing, such as curve jumping among others.

In this work, we propose a modified spherical algorithm (MSA) to path tracking of closed trajectories of the DBH method. There are several algorithms for path tracking homotopy curves, among them are the algorithms based on predictor and corrector steps, in which is situated the MSA algorithm. This algorithm proposes the use of hyperspheres to enclose homotopy trajectory combined with predictor and corrector steps, to allow the algorithm to follow the curve.

This paper is organized as follows. In Sect. 2 we explain the double-bounded homotopy method. In Sect. 3, the spherical method is explained. In Sect. 4, the strategy for avoiding the reversion phenomenon is proposed. Further, numerical examples are treated in Sect. 5. In Sect. 6, the results are discussed and finally the conclusions are given in Sect. 7.

2 Double-bounded homotopy

The DBH homotopy was proposed (Vazquez-Leal et al. 2005) as a homotopy that exhibits closed paths with the following formulation

$$H(f(x), \lambda) = C(\lambda - a)(\lambda - b) + \exp^{(\lambda-a)(\lambda-b)} \ln(D(F(x))^2 + 1), \tag{2}$$

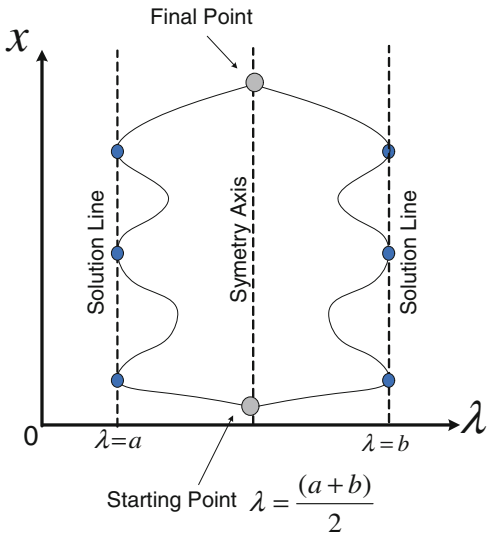

Fig. 1 DBH homotopy

where $F(x)$ is the original equation system, λ is the continuation parameter, and C and D are arbitrary positive constants. This homotopy contain two solution lines a and b; when both lines are applied to the homotopy, as a result the trajectory is forced to cross the double solution lines.

Figure 1 shows a trajectory with symmetrical branches and two solution lines. In Vazquez-Leal et al. (2005, 2013), how these characteristics can be used to establish a stop criterion for the homotopy simulation is explained. Different path-following techniques have been proposed for tracing the trajectories (Allgower and Georg 1994). Recently, Yamamura (1993) reported the spherical algorithm, which is easier to learn and implement than traditional methods (Allgower and Georg 1993, 1994; Watson et al. 1987; Vazquez-Leal et al. 2005, 2011; Bates et al. 2009, 2000, 2011).

3 The spherical algorithm

As aforementioned, the HCM methods require suitable path-tracking techniques to accurately trace the homotopy curves; otherwise, the homotopy simulation can miss solutions or not find any solution at all. On one side, the implementation of standard path-tracking techniques is a difficult task. On the order side, the spherical algorithm (SA) was proposed with a geometrically clear interpretation that eases the programming (Yamamura 1993).

The SA algorithm relies on the use of spheres for path tracking the homotopy curves. Such spheres are allocated over the homotopy trajectory, if the radius r of the spheres is where the sphere has two intersections above the curve (points o_2 y o_4) as shown in Fig. 2.

The homotopy formulation contains n equations and $n+1$ variables, where $x_i (i = 1, \ldots, n)$ represent the variables of the system and x_{n+1} is the homotopy parameter λ.

The equation that describes the sphere (Yamamura 1993; Vazquez-Leal et al. 2011) with center at c (initial point of the trajectory) and radius r is expressed by

$$S(X) = (x_1 - c_1)^2 + (x_2 - c_2)^2 + \cdots + (x_{n+1} - c_{n+1})^2 - r^2 = 0. \tag{3}$$

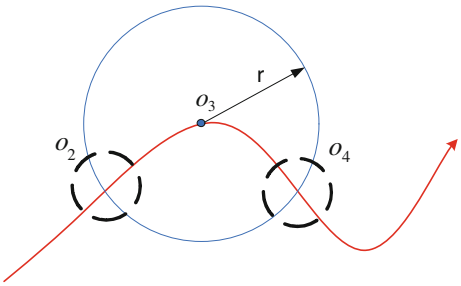

Fig. 2 Sphere intersecting with the curve at two points

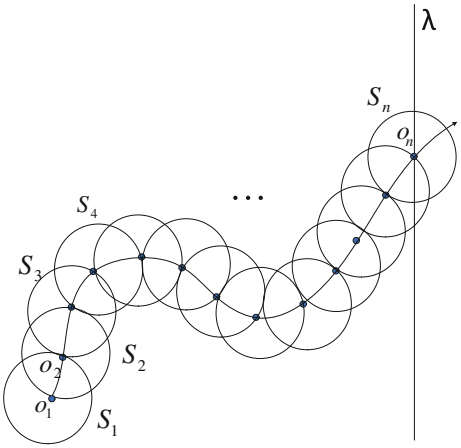

Fig. 3 Solution curves with spheres

Now, using (2) and (3), we formulated the augmented system as

$$\begin{aligned} &H_1(F_1(x), \lambda) = 0, \\ &H_2(F_2(x), \lambda) = 0, \\ &\vdots \\ &H_n(F_n(x), \lambda) = 0, \\ &S(x_1, x_2, \ldots, x_n, \lambda) = 0. \end{aligned} \tag{4}$$

The solution curve can be traced solving (4) for each sphere, updating the center of the hypersphere in each iteration step. The spheres $(S_1, S_2, \ldots)$ are allocated successively as shown in Fig. 3, and at each step the solution obtained is used as the center of the new sphere.

The proposed MSA scheme is described as follows:

- Predictor: The solving (4) point is located o_2 using the NR method setting o_1 as an initial point. The next predictor point is given using Fig. 4. Using the point o_1 as the center of the first sphere and o_2 as the center of the second sphere, prediction point is calculated by obtaining k_1. The last point will be used as initial point for the NR method until finding the point o_3 used as the center of the next sphere.
- Corrector: After calculating the point predictor, a point corrector is calculated by solving (4). It has at least two solutions: one lies in the forward direction (o_2) and the other in the backward direction (o_4) (see Fig. 2). If the radius of the sphere is small enough, then the task of distinguishing between the forward and backward solution is an issue due to numerical similarity. In Fig. 5, we can observe that the point predictor k_2 is used as an initial point for the NR; the method can locate the solution o_4 in the forward direction or

Fig. 4 Hyperspheres algorithm

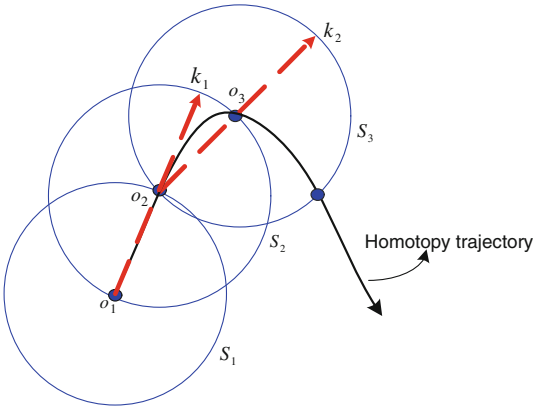

Fig. 5 Reversion solution

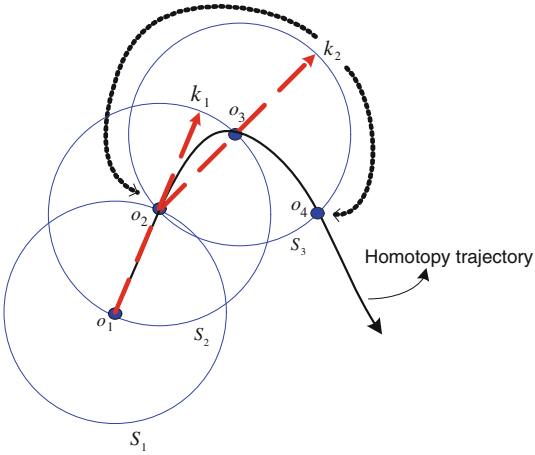

the solution o_2 in the backward direction. The forward solution can be considered as a success of the algorithm; nonetheless if the backward solution is obtained, the algorithm fails; such case of failure is known as "reversion" phenomenon of the MSA algorithm.

- Find zero strategy: The finding zero strategy should start after the trajectory bounces on the bounding line, because the DBH has a characteristic of never crossing $\lambda = 1$ (Sosonkina et al. 1996; Vazquez-Leal et al. 2005). A functional way consists of monitoring the change in sign of $\Delta\lambda$ after the corrector step. This procedure is realized by multiplying $\Delta\lambda$ of two consecutive predictor steps.

$$\text{sign}(\Delta\lambda_{j+1}\Delta\lambda_j) \tag{5}$$

The sign of $\Delta\lambda$ changes after bouncing from point k_1 to point k_2 as shown in Fig. 6, where $\Delta\lambda_j = k_2 - k_1$ and $\Delta\lambda_{j+1} = k_2 - k_3$.

- Interpolate solutions: When the trajectory bounces on the bounding line, the point (k_1, k_2) are taken to implement multidimensional interpolation to approximate the solution. Interpolation is performed using the command "ArrayInterpolation" (Maple program) as shown in Fig. 6.

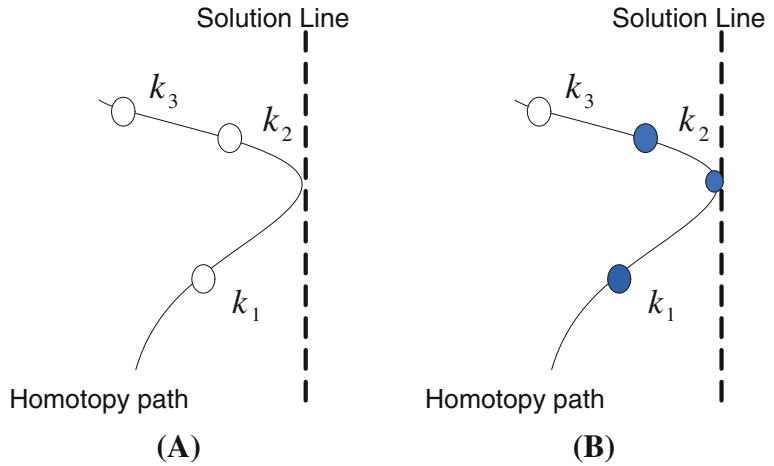

Fig. 6 **a** Solution bounce detection. **b** Interpolated solution

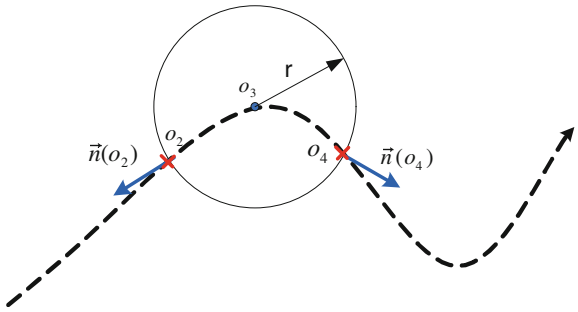

Fig. 7 Normal vector into the sphere

- Implicit accuracy for final solutions: The interpolated solution $\tilde{S}$ previously obtained has a low accuracy; therefore, the NR method is applied to obtain a solution with the required precision.

In the next section, we will propose a strategy to avoid the reversion phenomenon.

4 Strategy to avoid the reversion phenomenon

In Yamamura (1993), it was reported that using fixed radius for the spheres could aid in detecting the reversion phenomenon. Nonetheless, if the radius is small, the backward and forward solutions are really close numerically, making it difficult to differentiate between them. Therefore, we propose a strategy to compare the backward and forward solutions, avoiding the reversion problem.

As aforementioned, determining the difference between the forward direction o_4 and the backward direction o_2 is a difficult task. Therefore, calculating normal vector angles for the solution $(o_2,\ o_4)$ of the sphere o_2 and o_4 as depicted in Fig. 7. Firstly, we calculate the gradient of the sphere equation (3), resulting in

$$\nabla S = S'_{x_1}\hat{x_1} + S'_{x_2}\hat{x_2} + \cdots + S'_{\lambda}\hat{\lambda} \tag{6}$$

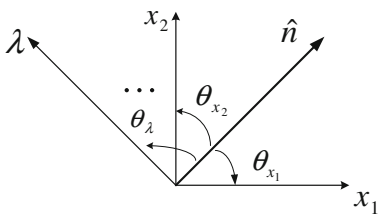

Fig. 8 Angle to normal vector

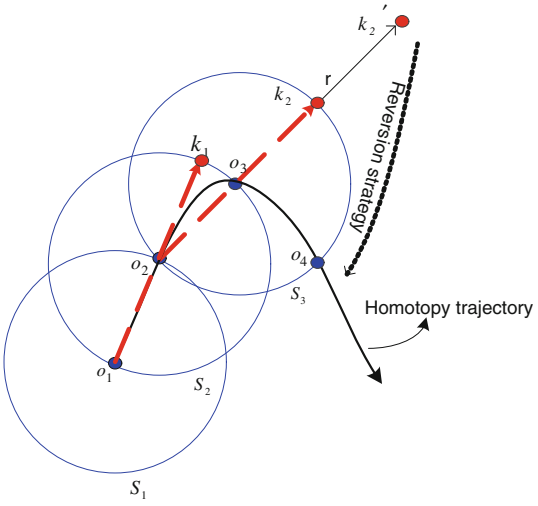

Fig. 9 Reversion strategy proposed

then the normal vector $\vec{n}$ is given by

$$\vec{n} = \frac{\nabla S}{\|\nabla S\|} \tag{7}$$

The notation $\|\nabla S\|$ represents the Euclidean norm of ∇S. Then the angle of $\vec{n}$ is obtained by calculating

$$\theta_{x_i} = \cos^{-1} \frac{S'_{x_i}}{\|\nabla S\|}, \quad i = 1, 2, \ldots, n+1 \tag{8}$$

where θ_{x_i} is the angle with respect to the coordinate axis, i corresponds to the number of system variables and $n + 1 = \lambda$. Figure 8 shows the normal vector to the sphere $\vec{n}$ with corresponding angles for each axis $(\theta_{x_1}, \theta_{x_2}, \ldots, \theta_\lambda)$.

Now, instead of comparing o_2 and o_4 directly, we use the angles of their normal vectors for an efficient comparison.

After detecting the reversion phenomenon, we have to modify the corrector step by increasing the radius a δr, inducing the corrector step to converge to the forward solution. Then, we propose the point $k_2 + \delta r$ that results in k_2' as the initial point for NR (see Fig. 9). This technique creates a perturbation in the corrector step that can induce the convergence to the forward solution. For this work, the step size takes values of δr which coincide with the sphere radius r.

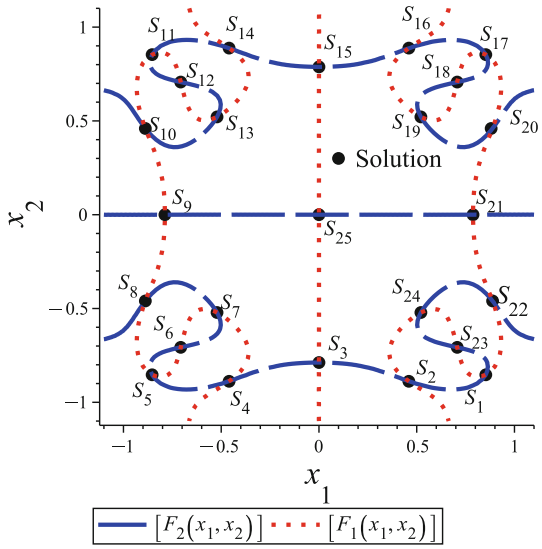

Fig. 10 Graphical solution of (9)

5 Numerical examples

To illustrate the reversion phenomenon and the proposed modifications for the spherical algorithm, two examples are presented.

5.1 Mathematical example

To show the proposed path-tracking algorithm, we will solve the following problem (Lee and Chiang 2001)

$$\begin{aligned} F_1(x_1, x_2) &= 4(x_1^2 + x_2^2 - 1)x_1 + 16((2x_1^2 - 1)^2 \\ &\quad +(2x_2^2 - 1)^2 - 2/3)(2x_1^2 - 1)x_1 = 0, \\ F_2(x_1, x_2) &= 4(x_1^2 + x_2^2 - 1)x_2 + 16((2x_1^2 - 1)^2 \\ &\quad +(2x_2^2 - 1)^2 - 2/3)(2x_2^2 - 1)x_2 = 0. \end{aligned} \tag{9}$$

Applying the DBH homotopy to (9), we obtain 7 solutions from a total of 25. Figure 10 shows a plot of the equations and location of the solutions (where $S_i, i = 1, 2, \ldots, 25$).

Applying the DBH homotopy, we obtain

$$\begin{aligned} &H_1(f_1, \lambda) = \lambda(\lambda - 1) + \exp(\lambda(\lambda - 1)) \ln(0.09((4v_1^2 + 4v_2^2 - 4)v_1 \\ &+16(2v_1^2 - 1)^2 + 16(2v_2^2 - 1)^2 - 32/3)(2v_1^2 - 1)v1)^2 + 1 = 0, \\ &H_2(f_2, \lambda) = \lambda(\lambda - 1) + \exp(\lambda(\lambda - 1)) \ln(0.09((4v_1^2 + 4v_2^2 - 4)v_2 \\ &+16(2v_1^2 - 1)^2 + 16(2v_2^2 - 1)^2 - 32/3)(2v_2^2 - 1)v2)^2 + 1) = 0, \\ &(v_1 - c_1)^2 + (v_2 - c_2)^2 + (\lambda - c_3)^2) = 0.0009. \end{aligned} \tag{10}$$

where the last equation corresponds to the sphere algorithm. The parameter homotopy $a = 0, b = 1, C = 3, D = 0.03$ and the ratio size is $r = 0.03$. Without a methodology for avoiding the reversion, the results are shown in Table 1, where in the first iteration $\lambda = 0.5$ and the second iteration λ goes back to $\lambda = 0.47$.

Table 1 Numerical results of path tracking in the backward direction

Iter.	x_1	x_2	λ	Angle(x_1)	Angle(x_2)	Angle(λ)
1	0.931862833	−0.931862833	0.5	90.2/90.2	89.7/89.7	179.5/179.5
2	0.931707573	−0.931707573	0.470000000	89.7/90.8	90.2/89.1	0.41/178
3	0.931242105	−0.931242105	0.440004014	89.1/91.4	90.8/88.	1.25/177.9

Table 2 Numerical results of path tracking in the forward direction

Iter.	x_1	x_2	λ	Angle(x_1)	Angle(x_2)	Angle(λ)
1	0.931862833	−0.931862833	0.5	90.2/90.2	89.7/89.7	179.5/179.5
2	0.931707573	−0.931707573	0.530000000	89.7/90.8	90.2/89.1	179.5/1.25
3	0.931242105	−0.931242105	0.559995985	91.4/89.1	90.8/88.5	178.7/2.09

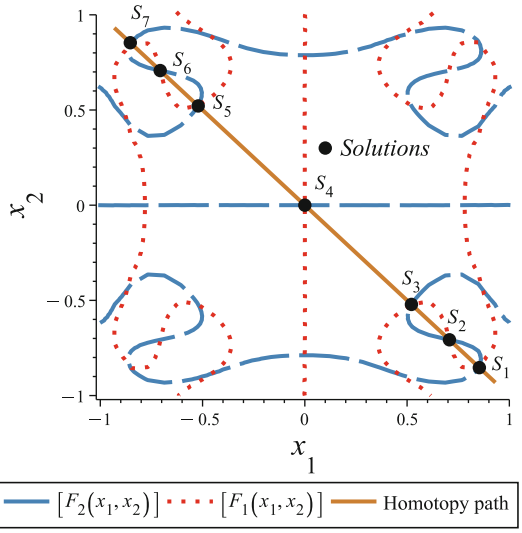

Fig. 11 Homotopy path for (10)

Table 2 shows the results after applying the reversion strategy proposed in this paper. The numerical solutions are shown in Table 2, where $\lambda = 0.5$ in the first iteration at the second iteration $\lambda = 0.53$ tracing the trajectory circumvent the reversion phenomenon.

The solutions S_1, S_2, S_3, S_4, S_5, S_6, S_7 found are shown in Fig. 11 traced with 119 iterations.

Table 3 shows solutions, accuracy and the number of iterations related to the path tracking of (10).

The projection of variable x_1 and x_2 over λ is shown in Fig. 12.

Table 3 Numerical solutions to the equation (10)

Solution	Iteration	v_1	v_2	Error $= \sqrt{f_1^2 + f_2^2}$
S_1	19	0.853356743	−.853356743	3E−15
S_2	26	0.707106781	−0.707106781	8.61E−14
S_3	34	0.521327409	−0.521327409	3.29E−11
S_4	61	−1.71E−16	1.70E−16	2.4E−11
S_5	87	−0.521327409	0.521327409	2E−15
S_6	96	−0.707106785	0.707106785	2E−15
S_7	103	−0.853356744	0.853356744	9.6E−11

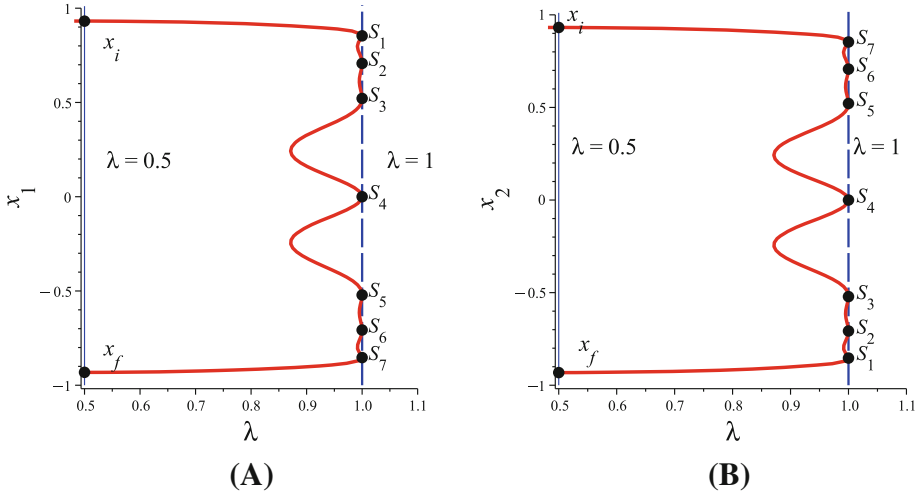

Fig. 12 **a** Homotopy path projected over x_1-λ. **b** Homotopy path projected over x_2-λ.

5.2 Circuit with two tunnel diodes

The following study case shows a circuit with two tunnel diodes, one voltage source and a resistor in series (see Fig. 13). The expression for the tunnel diode model is shown below

$$\begin{aligned} g_1(v_1) &= 2.5v_1^3 - 10.5v_1^2 + 11.8v_1, \\ g_2(v_2) &= 0.43v_2^3 - 2.69v_2^2 + 4.56v_2. \end{aligned} \tag{11}$$

Using Kirchoff laws, we obtain

$$\begin{aligned} F_1(v_1, v_2) &= E - Rg_1(v_1) - (v_1 + v_2) = 0, \\ F_2(v_1, v_2) &= g_1(v_1) - g_2(v_2) = 0. \end{aligned} \tag{12}$$

Applying the DBH homotopy to (12) results in

$$\begin{aligned} H_1(f_1, \lambda) = 40\lambda(\lambda - 1) + \exp(\lambda(\lambda - 1)) \ln(0.01(30 - 33.25v_1^3 \\ +139.65v_1^2 - 157.94v_1 - v_2)^2 + 1) = 0, \end{aligned}$$

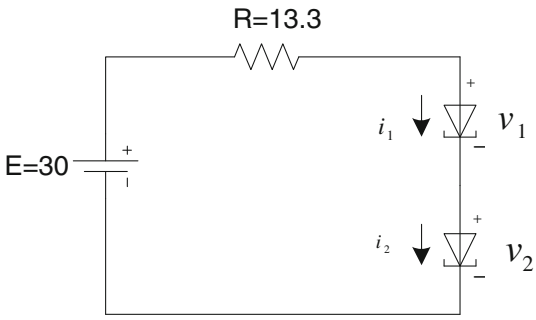

Fig. 13 Two tunnel diode circuit

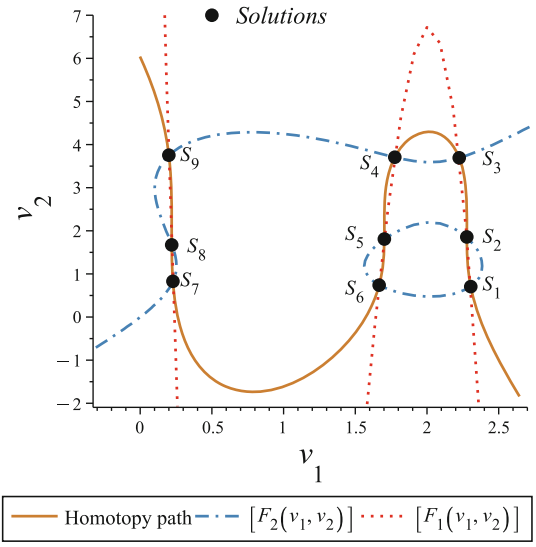

Fig. 14 Homotopy path for (13)

$$
\begin{aligned}
&H_2(f_2, \lambda) = 40\lambda(\lambda - 1) + \exp(\lambda(\lambda - 1)) \ln(0.01(2.5v_1^3 + 10.5v_1^2 \\
&+11.8v_1 - 0.43v_2^2 + 2.69v_2^2 - 4.56v_2)^2 + 1) = 0, \\
&(v_1 - c_1)^2 + (v_2 - c_2)^2 + (\lambda - c_3)^2) - 0.36 = 0.
\end{aligned} \tag{13}
$$

As a result of tracing the homotopy path, the nine operation points of the circuit have been located (see Fig. 14).

Table 4 shows the solutions found, iteration number for each solution and the error using mean squares.

5.3 Circuit with two-tunnel exponential diodes

For the diode circuit in Fig. 13, the polynomial expression is replaced by exponential terms

$$
i_{1,2} = I_p \left(\frac{V}{V_p} \right) \mathrm{e}^{1 - \frac{V}{V_p}} + I_0 \mathrm{e}^{\frac{q}{KT} V} \tag{14}
$$

where $E = 1$, $R = 20\Omega$, $I_p = 100\mathrm{E}{-}03$, $V_p = 50\mathrm{E}{-}03$, $I_0 = 1\mathrm{E}{-}09$ and $\frac{q}{KT} = 40$.

Table 4 Numerical solutions to the Eq. (13)

Solution	Iteration	v_1	v_2	Error $= \sqrt{f_1^2 + f_2^2}$
S_1	106	2.305222063	0.705560377	1.3E−10
S_2	143	2.277597006	1.857491731	3.3E−10
S_3	205	2.224729753	3.693043974	6.5E−10
S_4	249	1.775503561	3.707177714	8.8E−11
S_5	316	1.702657758	1.809029946	1.4E−10
S_6	349	1.666377840	0.739343469	5.8E−11
S_7	533	0.228266851	0.828626137	1.2E−11
S_8	558	0.219854573	1.672951409	1.03E−10
S_9	628	0.199790592	3.754217099	1.10E−11

Table 5 Numerical solutions for the circuit Fig. 13 with exponential terms

Solution	Iteration	I_{v_1}	v_2	v_3	Error $= \sqrt{f_1^2 + f_2^2}$
S_1	45	−0.048873941	0.022521177	0.011260588	1.1E−13
S_2	52	−0.042175710	0.156485795	0.147132103	6.5−10
S_3	70	−0.018919917	0.621601653	0.418182617	1.5−11
S_4	77	−0.028280221	0.434395575	0.428548398	2.4−11
S_5	80	−0.009914377	0.801712456	0.400856225	2.3−09

As a result, the path tracking shows the projection of I_{v_1}, v_2, v_3 over λ Table 5.

Figure 15 shows the projection I_{v_1}, v_2, v_3 over λ.

A standard path-tracking algorithm (Euler predictor and Newton corrector) will be used to solve the same problems and a comparison will be discussed. Table 6 concentrates on the results of all the cases studied.

6 Discussion

The obtained numerical results show that the MSA algorithm is useful to solve different problems containing polynomial and exponential terms. In the first case study, we obtained 7 from 25 possible solutions and for the second we found all the operating points of the circuit. However for the last case study, we only found five solutions, though it is the same circuit as for case study 2. This is mainly because of the highly nonlinear behavior of the exponential terms which causes numerical noise. The MSA algorithm is a suitable tool for following the homotopy trajectories. Additionally, we showed that the reversion phenomenon was successfully circumvented. The angles of the normal vector show that the reversion problem can be detected using the proposed methodology. The angles calculated for the normal vector Fig. 8 are the same for the first iteration as shown in Table 1, indicating that the backward solution has been found. For the second iteration, the trajectory carries a backward direction. The same results are shown in Table 2 for the first iteration; however the strategy proposed in this work has been applied achieving a difference between the angles of even 180 ° for the second iteration. The above allows a tracing of the curve in the forward direction. The strategy to circumvent reversion was successful in the case studies presented in this work; nonetheless, other case studies might need other radius values to cause perturbation.

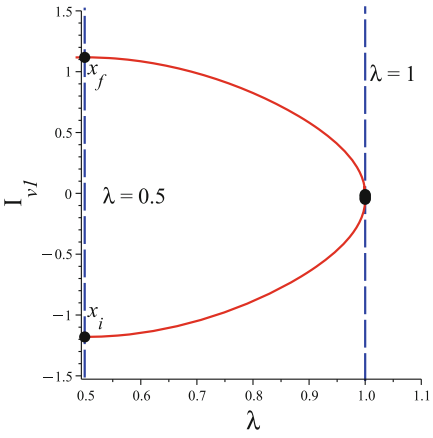

(a) Homotopy path proyected over I_{v_1}-λ

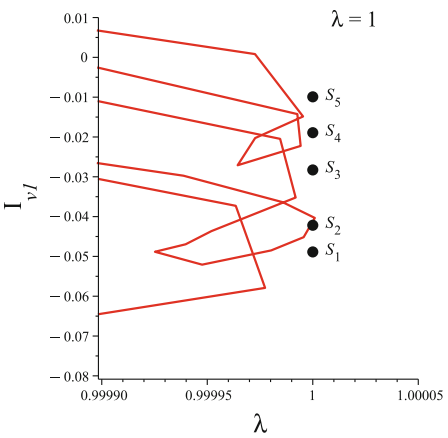

(b) Zoom to solutions of (a)

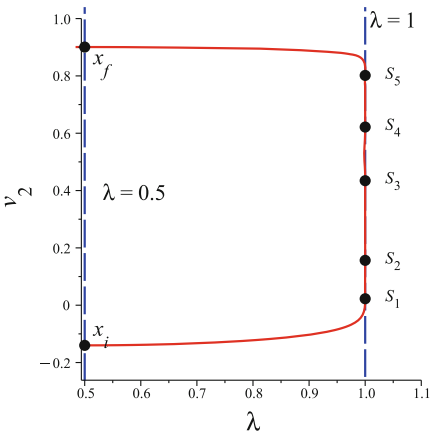

(c) Homotopy path proyected over v_2-λ

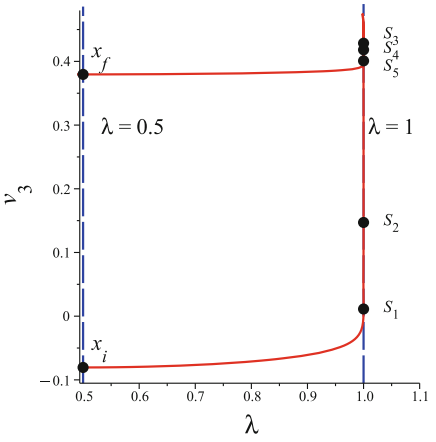

(d) Homotopy path proyected over v_3-λ.

Fig. 15 The projection I_{v_1}, v_2, v_3 over λ

The results in Table 6 show that the path tracking is similar for both methods because the initial point and the final points are numerically similar. As a future work, the MSA algorithm will be tested for the simulation of VLSI circuits. Such test will show the behavior of the proposed algorithm when large NAEs are solved. Radio size must be variable following the behavior of the curve in each step in the path. The CPU time between the standard algorithm (based on an Euler predictor and a Newton corrector) and the proposed method shows good agreement with slightly shorter CPU time for the standard algorithm; however, the programming for MSA method is easier to implement. Finally, the reversion strategy used for all examples was successful for all case studies. Nevertheless, to decrease the simulation time, the corrector step should be optimized.

Table 6 Comparative results for all study cases

	Spherical method		Euler method
Case study 1	Initial point	$x_1 = 0.93186283$, $x_2 = -0.93186283$	$x_1 = 0.93186283$, $x_2 = -0.93186283$
	Step size	0.03	0.03
	Iteration number	119	119
	Solutions	7	7
	CPU time	1.1	0.98
	C, D	3,0.03	3,0.03
	Reversion strategy	1	–
	Final point	$x_1 = -0.931803691$, $x_2 = 0.931803691$	$x_1 = -0.931862024$, $x_2 = 0.931862024$
Case study 2	Initial point	$x_1 = -0.00160602$, x_2 =6.04189368,	$x_1 = -0.00160602$ x_2 =6.04189368
	Step size	0.03	0.03
	Iteration number	722	722
	Solutions	9	9
	CPU time	5.7	4.1
	C, D	6,0.01	6,0.01
	Reversion strategy	1	–
	Final point	$x_1 = -0.065939784$,	$x_1 = -0.0659397464$,
	Final point	$x_2 = 6.4852273$	$x_2 = 6.48522706$
Case study 3	Initial point	$x_1 = -1.18026447$, $x_2 = -0.14007670$, $x_3 = -0.08050098$	$x_1 = -1.18026447$, $x_2 = -0.14007670$, $x_3 = -0.08050098$
	Step size	0.03	0.03
	Iteration number	123	123
	Solutions	5	5
	CPU time	2.6	1.1
	C, D	1,0.3	1,0.3
	Reversion strategy	1	–
	Final point	$x_1 = 1.117427493$,	$x_1 = 1.11215323$
	Final point	$x_2 = 0.900653843$,	$x_2 = 0.900567747$,
	Final point	$x_3 = 0.379577056$	$x_3 = 0.379608015$

7 Conclusions

The MSA algorithm was adapted to the tracing of DBH homotopy. Using three examples of different nature (including exponential or polynomial terms), we showed how the MSA algorithm was able to trace the closed paths and locate multiple solutions. In addition, the strategy for circumventing the reversion phenomenon was tested, reaching good results. What is more, we compared the proposed algorithm with a standard one reaching a good agreement between the results of both techniques. Finally, further work should be developed to test the MSA algorithm by applying it to larger circuits.

Acknowledgments The first author is grateful to CONACYT for financial support through scholarship 204402. The second author gratefully acknowledge the financial support provided by the National Council for Science and Technology of Mexico (CONACyT) through Grant CB-2010-01 no. 157024.

References

Allgower EL, Georg K (1993) Continuation and path following. Acta Numerica 2:1–64
Allgower E, Georg K (1994) Numerical path following. Department of Mathematics, Colorado State University

Bates DJ, Hauenstein JD, Sommese AJ, Wampler CW II (2000) Adaptive multiprecision path tracking. SIAM J 46(2):722–746
Bates DJ, Hauenstein JD, Sommese AJ, Wampler CW (2009) Stepsize control for adaptive multiprecision path tracking. Contemp Math 496:21–31
Bates DJ, Hauenstein JD, Sommese AJ (2011) Efficient path tracking methods. Numer Algorithms 58(4):451–459
Dyes A, Chan E, Hofmann H, Horia W, Trajkovic L (1999) Simple implementations of homotopy algorithms for finding DC solutions of nonlinear circuits. ISCAS 6:290–293
Lee J, Chiang H-D (2001) Constructive homotopy methods for finding all or multiple DC operating points of nonlinear circuits and systems. IEEE Trans Circuits Syst I Fundam Theory Appl 48(1):35–50
Melville RC, Trajkovic L, Fang SC, Watson LT (1993) Artificial parameter homotopy methods for the DC operating point problem. IEEE Trans CAD Integr Circuits Syst 12(6):861–877
Melville RC, Trajkovic L, Fang S-C, Watson LT (1993) Artificial parameter homotopy methods for the DC operating point problem. IEEE Trans Comput Aided Des Integr Circuits Syst 12(6):861–877
Ogrodzki J (1994) Circuit simulation: methods and algorithms, vol 5. CRC Press, Boca Raton
Sosonkina M, Watson LT, Stewart DE (1996) Note on the end game in homotopy zero curve tracking. ACM Trans Math Softw 22(3):281–287
Vazquez-Leal H, Hernandez-Martinez L, Sarmiento-Reyes A, Castaneda-Sheissa R, Gallardo-Del-Angel A (2011) Homotopy method with a formal stop criterion applied to circuit simulation. IEICE Electron Express 8(21):1808–1815
Vazquez-Leal H, Hernandez-Marin A, Khan Y, Yildirim A, Filobello-Nino U, Castaneda-Sheissa R, Jimenez-Fernandez VM (2013) Exploring collision-free path planning by using homotopy continuation methods. Appl Math Comput 219(14):7514–7532
Vazquez-Leal H, Castaneda-Sheissa R, Rabago-Bernal F, Hernandez-Martinez L, Sarmiento-Reyes A, Filobello-Nino U (2011) Powering multiparameter homotopy-based simulation with a fast path-following technique. ISRN Appl Math 2011, Art. ID 610637
Vazquez-Leal H, Castaneda-Sheissa R, Yildirim A, Khan Y, Sarmiento-Reyes A, Jimenez-Fernandez V, Herrera-May AL, Filobello-Nino U, Rabago-Bernal F, Hoyos-Reyes C (2012) Biparameter homotopy-based direct current simulation of multistable circuits. Br J Math Comput Sci 2(3):137–150
Vazquez-Leal H, Hernandez-Martinez L, Sarmiento-Reyes A (2005) Exploring collision-free path planning by using homotopy continuation methods. In: IEEE International Symposium on Circuits and Systems, 2005 (ISCAS 2005), vol 4, pp 3203–3206
Vazquez-Leal H, Hernandez-Martinez L, Sarmiento-Reyes A, Castaneda-Sheissa R (2005) Numerical continuation scheme for tracing the double bounded homotopy for analysing nonlinear circuits. In: Proceedings 2005 International Conference on Communications, Circuits and Systems, vol 2
Vazquez-Leal H, Sarmiento-Reyes A, Filobello-Nino U, Khan Y, Herrera-May AL, Castaneda-Sheissa R, Jimenez-Fernandez VM, Vargas-Dorame M, Sanchez-Orea J (2013) A homotopy continuation approach for testing a basic analog circuit. Br J Math Comput Sci 226–240
Vazquez-Leal H, Sarmiento-Reyes A, Khan Y, Yildirim A, Filobello-Nino U, Castaneda-Sheissa R, Herrera-May AL, Jimenez-Fernandez VM, Hernandez-Machuca SF, Cuellar-Hernandez L (2013) New aspects of double bounded polynomial homotopy. Br J Math Comput Sci (in press)
Watson LT, Billups SC, Morgan AP (1987) Algorithm 652: HOMPACK: a suite of codes for globally convergent homotopy algorithms. ACM Trans Math Softw 13(3):281–310
Watson LT, Sosonkina M, Melville RC, Morgan AP, Walker HF (1997) Algorithm 777: HOMPACK90: a suite of Fortran 90 codes for globally convergent homotopy algorithms. ACM Trans Math Softw 23(4):514–549
Wolf DM, Sanders SR (1996) Multiparameter homotopy methods for finding DC operating points of nonlinear circuits. IEEE Trans Circuits Syst I Fundam Theory Appl 43(10):824–838
Wu TM (2006) Solving the nonlinear equations by the Newton-homotopy continuation method with adjustable auxiliary homotopy function. Appl Math Comput 1773(1):383–388
Yamamura K (1993) Simple algorithms for tracing solution curves. IEEE Trans Circuits Syst I Fundam Theory Appl 40(8):537–541
Yamamura K, Sekiguchi T, Inoue Y (1999) A fixed-point homotopy method for solving modified nodal equations. IEEE Trans Circuits Syst I Fundam Theory Appl 46(6):654–665